ISSN 1027-4510, Journal of Surface Investigation. X-ray, Synchrotron and Neutron Techniques, 2015, Vol. 9, No. 5, pp. 984–994. © Pleiades Publishing, Ltd., 2015.

The Optically Induced and Bias-Voltage-Driven Magnetoresistive Effect in a Silicon-Based Device[1]

N. V. Volkov[a, b], A. S. Tarasov[a, b], M. V. Rautskii[a], A. V. Lukyanenko[a, b], F. A. Baron[a], I. A. Bondarev[a, b], S. N. Varnakov[a, c], and S. G. Ovchinnikov[a, b]

[a] *Kirensky Institute of Physics, Russian Academy of Sciences, Siberian branch, Krasnoyarsk, 660036 Russia*
[b] *Siberian Federal University, Institute of Engineering Physics and Radio Electronics, Krasnoyarsk, 660041 Russia*
[c] *Siberian State Aerospace University, Institute of Space Technology, Krasnoyarsk, 660014 Russia*
e-mail: volk@iph.krasn.ru

Received March 3, 2015

Abstract—The giant change in photoconductivity of a device based on the Fe/SiO_2/*p*-Si structure in magnetic field is reported. As the magnetic field increases to 1 T, the conductivity changes by a factor of more than 25. The optically induced magnetoresistance effect is strongly dependent of the applied magnetic field polarity, as well as of sign and value of a bias voltage across the device. The main mechanism of the magnetic field effect is related to the Lorentz force, which deflects the trajectories of photogenerated carriers, thereby changing their recombination rate. The structural asymmetry of the device leads to the asymmetry of the dependence of recombination on the magnetic field polarity: recombination of carriers deflected in the bulk of semiconductor is relatively slow, while recombination of carriers at the SiO_2/*p*-Si interface is faster. In the latter case, the interface states serve as effective recombination centers. The bias voltage sign specifies the type of carriers, whose trajectories pass near the interface, providing the main contribution to the magnetoresistance effect. The bias voltage controls the electric field accelerating carriers and, thus, affects the hole and electron trajectories. Moreover, when the bias voltage exceeds a certain threshold value, the electron impact ionization regime is implemented. The magnetic field suppresses impact ionization by enhancing recombination, which makes the largest contribution to the magnetoresistance of the device. The investigated device can be used as a prototype of silicon chips controlled simultaneously by optical radiation, magnetic field, and bias voltage.

Keywords: magnetoresistance, magnetotransport properties, photoconductivity, bias voltage

DOI: 10.1134/S1027451015050432

INTRODUCTION

The giant magnetoresistive (GMR) effects observed in many new materials and artificial structures have been in focus of the global research community, since they give rise to the numerous fundamentally new physical problems. Solving these problems will open a wide spectrum of opportunities to integrate magnetoresistance functionalities into electronic devices. The magnetoresistive (MR) effects are applied in sensors, nonvolatile memory [1], and magnetologic electronics [2]. Some MR-based systems have the high potential for application in frequency synthesizers [3] and microwave detectors [4].

The MR effects are governed by different physical mechanisms. In particular, the GMR of bulk manganite crystals is due to the effect of magnetic phase separation [5], while in spin valves and tunneling structures it originates from the spin-dependent scattering and tunneling phenomena [6, 7]. Sometimes, the MR effects are observed only under an ac current bias. In soft magnetic ribbons and films, the ac MR effect originates from the magnetic field dependence of the skin depth [8]. The ac MR effect in sandwiched films is caused by the ac density redistribution over the film cross section in a magnetic field [9, 10]. The magnetic-field sensitivity of recharging of the interface states is responsible for magnetoimpedance in the metal/insulator/semiconductor (MIS) hybrid structures with the Schottky barrier [11].

In general, hybrid structures consisting of conventional semiconductors and magnetic materials appeared quite fruitful objects for studying the MR phenomenon originating from the spin-dependent transport [12]. The mechanisms underlying the MR effects in the hybrid structures are spin injection into a semiconductor, including the spin-polarized charge injection from ferromagnetic layers [13] and optically assisted spin injection [14], spin accumulation, spin diffusion, and detection.

[1] The article is published in the original.

In addition, the GMR effects were observed in nonmagnetic semiconductor structures. Some MR phenomena are related to the possibility of manipulating spin-polarized currents induced by the spin-orbit (SO) interaction, specifically, the spin Hall [15], Rashba [16], and Dresselhaus effects [17]. The spin Hall effect is caused by coupling the charge and spin currents due to spin-orbit interaction. The latter deflects the currents of the spin up and spin down channels in the opposite directions, thus inducing the spin current in a nonmagnetic material. The Rashba effect ensures an alternative way to create spin polarization of carriers due to the SO coupling in the structures that lack inversion symmetry. In this case, electrons moving in an asymmetric crystal field experience a net electric field, which transforms to a magnetic field in the electron's rest frame and effectively couples the spin to the electron orbital motion. The similar mechanism yet based on the Dresselhaus SO coupling rather than on the Rashba effect was described in [18].

The other group of the MR phenomena is related to the Lorentz force that acts on energetic carriers. In an applied magnetic field, the Lorentz force deflects the carrier trajectories in a specific direction. If a host semiconductor has some structural asymmetry, then the processes of recombination, scattering, and impact ionization can be substantially different for carriers moving along different trajectories, which ultimately results in the MR effect [19, 20]. The effect of a magnetic field on the transport properties of structurally uniform semiconductors at high bias voltages is mainly due to the carrier trajectory variations in a magnetic field; however, the space-charge inhomogeneity induced by a high electric field is of fundamental importance [21, 22].

At present, particular attention is focused on the MR effects sensitive to the magnetic field polarity, since they are interesting for both fundamental research and application in spintronic devices. The authors of study [20] consider these effects to be a simple and compact platform for non-volatile magnetic-field-controlled reconfigurable logic devices. It was established that the sensitivity of the MR effect to the field sign is related to the Lorentz force [19, 20]. However, the structures characterized by the Rashba (Dresselhaus) effect can also exhibit the field sign-dependent transport due to asymmetry of the electron spin distribution in the k space. In addition, there could be other mechanisms. In our previous study [23], we fabricated and investigated a simple planar device based on the $Fe/SiO_2/p$-Si hybrid structure, which exhibits the MR effect highly sensitive to the magnetic field sign. Interestingly, the large dc MR effect was observed only under the nonequilibrium conditions ensured by optical radiation.

There have been many attempts to govern the magnetoresistive properties of magnetic and hybrid structures by optical pumping. When studying the magnetic tunneling structure $La_{0.7}Sr_{0.3}MnO_3$/depletion manganite layer/MnSi, we observed that the optical excitation strongly affects the tunnel MR [24]. Although this effect is not explained just by heating and is related rather to generation of electron-hole pairs in the dielectric layer, which serves as a potential barrier, the MR ratio can only decrease with increasing optical power. An increase in the MR ratio under optical radiation was observed in the manganite/oxide/n-Si junction [25]. In this case, the effect of light was attributed to the additional contribution of photogenerated (spin-polarized) electrons to the tunnel current.

Regarding the photoinduced MR effect in the $Fe/SiO_2/p$-Si-based device, we suggest the observed phenomenon to be caused by a few physical mechanisms, which require further investigations. It still remains unanswered which mechanism is responsible for the high sensitivity of the transport properties of the device to the magnetic field polarity. Here, we report new experimental results in attempt to clarify the nature of the photoinduced MR effect sensitivity to the sign of a magnetic field applied to the $Fe/SiO_2/p$-Si structure-based device.

EXPERIMENTAL

The sample to investigate was the MIS Schottky diode based on the $Fe/SiO_2/p$-Si structure. The $Fe/SiO_2/p$-Si structure was formed on a p-Si wafer with a resistivity of 5 Ω cm and a doping density of 2×10^{15} cm^{-3}. The SiO_2 layer was chemically deposited onto the p-Si wafer surface and the iron thin film was formed by thermal evaporation. The SiO_2 and Fe layer thicknesses were 1.2 and 5 nm, respectively. The structure fabrication was described in more detail in [26].

The device topology and measurement setup are illustrated in the inset in Fig. 1a. The transport properties of the device were studied in the two-probe configuration. The Fe electrode in the form of a narrow strip 0.5×3 mm^2 in size was formed from a continuous iron film by wet etching on the structure's surface 3×3.5 mm^2 in size. The top contact to the Fe electrode was formed from the two-component silver epoxy adhesive. The indium ohmic contact was formed on the back (Si) substrate surface. To ensure a good ohmic contact, the native oxide layer was removed from the back surface and then the indium contact was formed by manual rubbing of indium alloy bits in silicon.

The transport properties were studied on an original facility comprising a helium cryostat, an electromagnet, and a KEITHLEY-2400 current/voltage source meter. Resistivity measurements were performed in a dc mode at a fixed voltage. The I–V characteristics were obtained in a voltage scanning mode. An external magnetic field was applied in the structure plane. The magnetoresistance was measured in fixed magnetic field and upon field sweeping from –1 to 1 T.

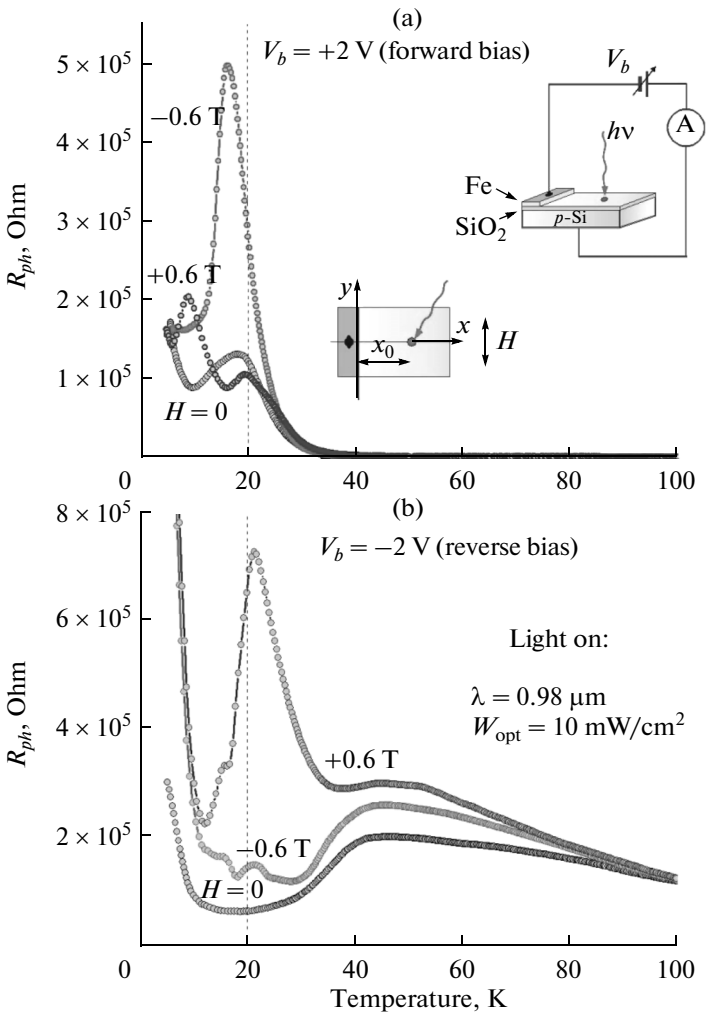

Fig. 1. Temperature dependence of resistance R_{ph} of the optically irradiated device at (a) forward bias ($V_b = +2$ V) and (b) reverse bias ($V_b = -2$ V) in zero magnetic field and in fields of +0.6 and −0.6 T. Inset: schematics of the device topology and measurement setup.

The optical excitation source was a laser diode with a wavelength of 980 nm ($h\nu = 1.26$ eV). The sample was exposed to linearly polarized light with a power density of up to 10 mW/cm^2. In addition, we performed the measurements in circularly polarized light, yet found no difference in the experimental data obtained at different light polarizations. The laser was focused to a 0.5-mm spot on the structure's surface in the place where the Fe layer was removed. The spot position in the experiments was varied.

RESULTS AND DISCUSSION

First, we present the measured magnetotransport properties of the optically irradiated sample. The sample geometry is shown in the inset in Fig. 1a. The laser spot was localized at the distance $x_0 = 1.25$ mm from the metal electrode and at the device midpoint relative to its long sides, i.e., along the x axis. Magnetic field H was applied in the structure plane along the Fe strip, i.e., the y axis. Figure 1 shows the temperature dependence of resistance R_{ph} of the optically irradiated device at $H = 0$ and in the magnetic fields $H = \pm 0.6$ T of the opposite polarities. The dependences in Fig. 1a are consistent with the data measured at the forward bias voltage across the MIS Schottky diode ($V_b > 0$, the negative potential is on the Fe electrode). The data obtained at the reverse bias ($V_b < 0$) are shown in Fig. 1b. The noticeable variation in the transport properties is observed in a magnetic field at temperatures below 100 K. The R_{ph} value changes the most in the temperature range 10–40 K, where the MR effect is the most sensitive to the magnetic field polarity. At the forward bias, R_{ph} changes insignificantly in the field $H = +0.6$ T; in the field of the inverse polarity ($H = -0.6$ T) the resistance variation is much more pronounced. In the latter case, we observe a peak in the $R_{ph}(T)$ curve in the range 10–30 K. In the vicinity of this peak in the field $H = -0.6$ T R_{ph} increases by a factor of almost 5, i.e., the relative resistance change referred to as the magne-

toresistance $MR_{ph} = 100\%(R_{ph}(H) - R_{ph}(0))/R_{ph}(0)$ amounts to approximately 300%. Under the reverse bias conditions, i.e., at $V_b < 0$, the dependence of R_{ph} on the magnetic field polarity is reversed (Fig. 1b): the magnetic field effect is weaker in the field $H = -0.6$ T than in the field $H = +0.6$ T and the intense characteristic peak arises in the $R_{ph}(T)$ dependence again. The shape of this peak is somewhat different from that observed at the forward bias and its maximum is shifted by about 5 K toward higher temperatures. In the field $H = +0.6$ T, the resistance at the peak maximum is increased by a factor of more than 11 and the MR_{ph} value attains 1000%. Thus, in the reverse- biased structure, the MR effect values are larger than at the forward bias. Another feature of the $R_{ph}(T)$ curve at $V_b < 0$ is the sharp R_{ph} growth at temperatures below 10 K, which is observed even at $H = 0$ and especially pronounced in nonzero field of any polarity.

The main features in the behavior of the $R_{ph}(T)$ curve below 40 K can be interpreted in terms of the dynamics of surface states, which are localized at the oxide-semiconductor interface and strongly affect the transport properties of the structure. The presence of such states and their in-gap energy spectra were established by us previously [11]. As the temperature is decreased, the Fermi energy level (E_F) in p-type semiconductor shifts toward the top of the valence band and at 40 K crosses the energy levels of the interface centers. As a result, these centers start releasing electrons and effectively contributing to the generation-recombination processes. They also provide additional tunneling paths between the metal and semiconductor, which changes the transport properties of the structure. Below we consider the energy band diagram and discuss the fundamental carrier transport processes involving the interface states under laser radiation at the forward and reverse bias on the structure.

Figure 2 shows the bias voltage dependence of the transport and magnetotransport properties of the optically excited device. It is noteworthy that at temperatures above 40 K, the I–V characteristics are typical of the MIS tunnel diode (see inset in Fig. 2a) even under optical radiation. Such a behavior of the I–V characteristics of the diode can be explained within the classical approach, which takes into account the transition of the semiconductor surface from depletion to accumulation upon bias sweep and ignores the presence of surface states [27]. However, below 40 K, the behavior of the I–V curves drastically changes even in zero magnetic field. We believe that it is the contribution of the filling factor, recombination-generation, and tunneling dynamics of the interface states that complicates the behavior of the photocurrent upon variation in V_b. Figure 2a presents the I–V characteristics of the optically irradiated device at $T = 20$ K in the fields $H = 0$ and $H = \pm 0.8$ T. It can be seen that the magnetic field not only reduces the photocurrent value at all applied biases V_b, but also modifies the shape of the I–V curves. At all biases V_b, the current is highly sensitive to the magnetic field polarity. As we mentioned above, the photocurrent at the forward and reverse bias changes the most in the applied magnetic field of the opposite polarities.

Figure 2b shows the bias voltage dependence of the MR ratio of the irradiated structure at $H = +0.8$ and -0.8 T. Except for the small bias region form -1 V to $+1$ V, where MR_{ph} sharply changes, one can see that an increase in the forward bias leads to the MR_{ph} drop, and the difference between the MR ratios corresponding to the opposite field polarities increases. On the contrary, an increase in the reverse bias leads to the MR_{ph} growth, and the difference between the MR ratios corresponding to the opposite field polarities decreases.

The magnetic field dependences of the resistance $R_{ph}(H)$ presented in Fig. 3 show that not only the MR_{ph} values but also the character of the $R_{ph}(H)$ dependences are different for the forward and reverse biases across the device. At $V_b > 0$ (Fig. 3a), for one of the field polarities, the R_{ph} value first decreases and then, at a certain H value, starts growing. At $V_b < 0$ (Fig. 3b), the minimum R_{ph} value corresponds to zero magnetic field and the resistance increases at any field polarity. It should be noted that at a fixed temperature the shape of the $R_{ph}(H)$ curve remains invariable at any applied bias V_b of one sign and only the R_{ph} value changes.

As the temperature is decreased, the $R_{ph}(H)$ dependences become more complex at both the forward and reverse bias across the structure. This reflects the complexity of the magnetic field effect on the transport properties of the investigated device under illumination. In our opinion, a few physical mechanisms might underlie the response of the transport properties to an external magnetic field. These mechanisms apparently originate from the presence of surface states, their in-gap density distribution, features of their energy structure, and its possible modification under the action of an external magnetic field. However, the field effect consists mainly in changing the trajectories of electrons and holes excited by light near the SiO_2/p-Si interface where the interface states are localized, which, in turn, can work as recombination centers. This explains the strong dependence of the transport properties on the filed polarity.

The mechanism of carrier trajectory change in a magnetic field is indirectly confirmed by the high sensitivity of the MR effect to the light spot position on the sample's surface relative to the metal electrode (x_0 in the inset in Fig. 1a). Since the photocurrent depends on the carrier lifetime, it increases at all V_b values with decreasing x_0. It appeared, however, that in this case the MR_{ph} value decreases. Figure 4 shows the $MR_{ph}(H)$ dependences for $x_0 = 1$ and 0.25 mm. A decrease in the MR effect value with decreasing x_0 can be clearly seen at the reverse bias across the structure, when the MR effect is pronounced much stronger

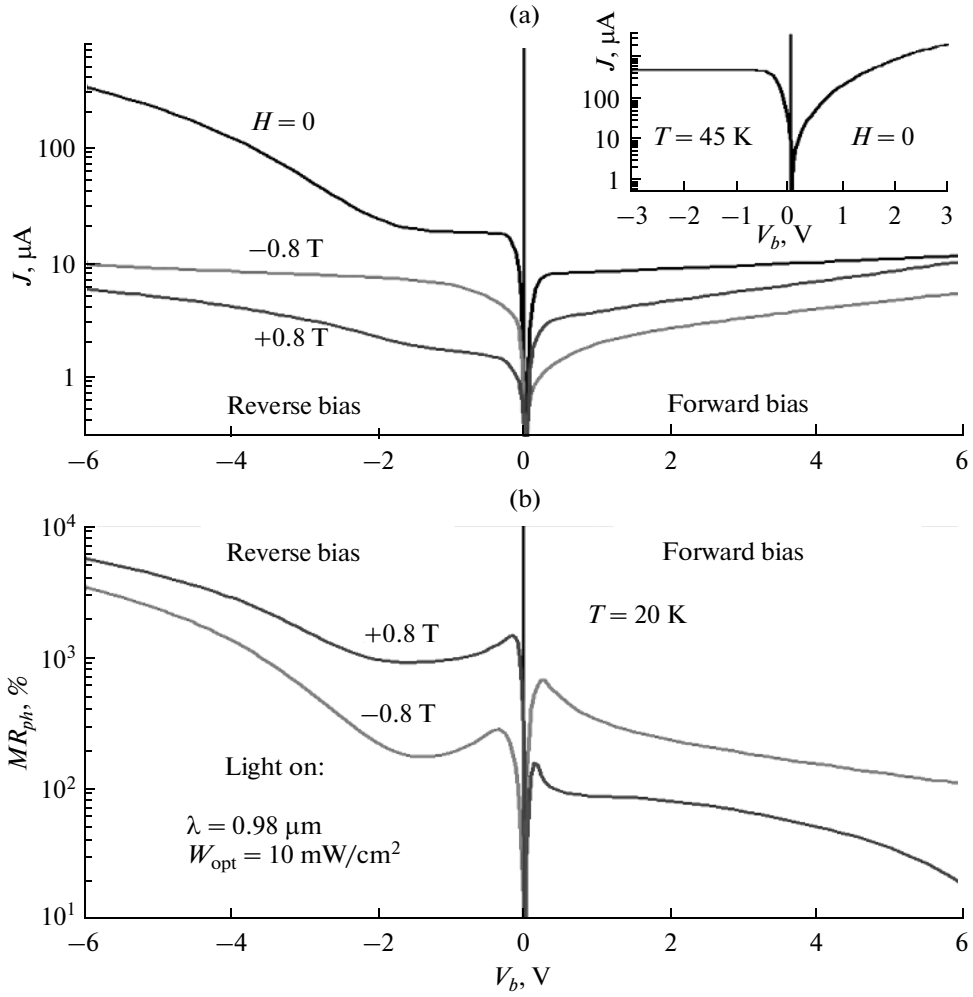

Fig. 2. (a) I–V characteristics of the optically irradiated device at $H = 0$ and in fields of H of +0.8 and −0.8 T at $T = 20$ K. Inset: I–V characteristic under optical radiation at $T = 45$ K and $H = 0$. (b) Magnetoresistance MR_{ph} vs bias voltage at $H = +0.8$ and −0.8 T.

than at the forward bias, at all other factors being the same. In the magnetic field range from −1 and +1 T, the MR_{ph} value decreases by a factor of 4–5 in the negative fields and by a factor of 7–9 in the positive fields. In the forward-biased structure, a decrease in MR_{ph} in the negative field is not as strongly pronounced. Moreover, at the positive field polarity we can no longer speak about a decrease in MR_{ph}, since here the effect has different signs, but the integral MR ratio changes in a field increasing from 0 to +1 T are similar. Note, however, that at $V_b > 0$, the observed MR_{ph} values are smaller than those at $V_b < 0$ by more than an order of magnitude.

Although we stated that the observed MR effect is related to the presence of the interface states and to deflection of the carrier trajectories, let us analyze the models describing the magnetic-field effect in semiconductors and semiconductor-based devices. First, note that, in contrast to all the well-studied MR effects observed in nonmagnetic semiconductors and hybrid structures, the MR effect investigated by us is implemented only under optical excitation, i.e., is related to photogenerated nonequilibrium electron-hole pairs. Therefore, we believe that the mechanism underlying the phenomenon observed by us differs from the mechanism implemented in lightly doped semiconductors in the hopping conductivity mode, which is related to shrinking the wave function of the impurity state in strong magnetic fields [28].

The large positive MR is characteristic also of inhomogeneous semiconductors. Linear or quadratic positive MR is caused by the distortions of current paths in a magnetic field due to the inhomogeneity [29]. The inhomogeneity of both the carrier density and carrier mobility can be induced by injection of electrons or holes into a semiconductor [21]. In addition, the MR value is affected by the chosen device geometry. However, the main underlying mechanism is still the spatial variation in carrier mobility [22]. We do not consider the inhomogeneity-induced MR mechanism to be applicable in our case. First, the $MR_{ph}(H)$ dependences obey neither linear nor qua-

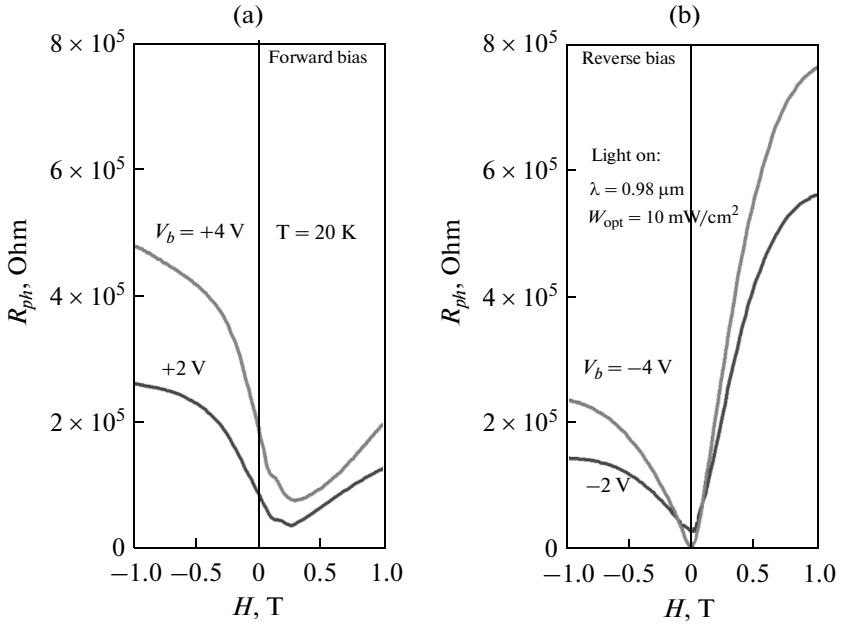

Fig. 3. Resistance R_{ph} of the optically irradiated device as a function of magnetic field at $T = 20$ K and (a) forward biases of +2 and +4 V and (b) reverse biases of −2 and −4 V.

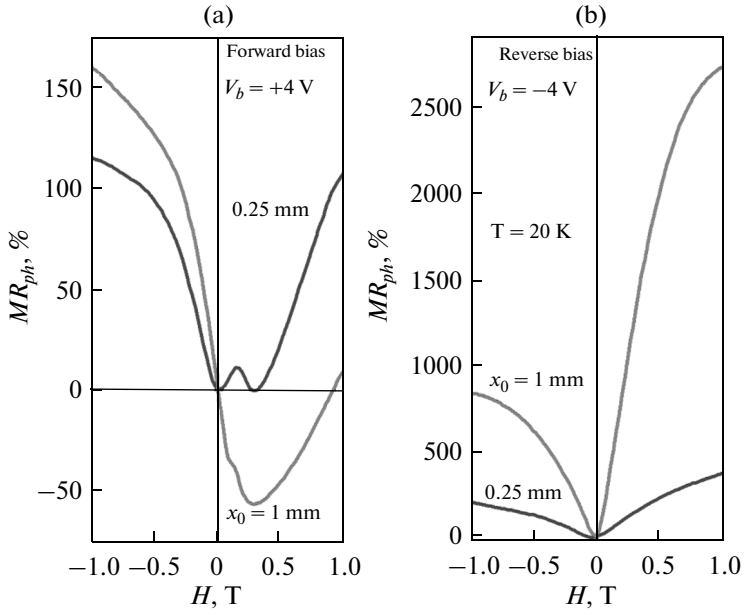

Fig. 4. Magnetoresistance MR_{ph} vs magnetic field for two laser spot positions on the device's surface relative to the Fe electrode, $x_0 = 1$ and 0.25 mm (see inset in Fig. 1) at (a) a forward bias of +4 V and (b) a reverse bias of −4 V at a temperature of 20 K.

dratic law and exhibit a complex nonmonotonic behavior, containing both positive and negative MR portions. The high sensitivity of the resistance to the field polarity cannot be explained within this mechanism either.

Let us consider another group of the large MR effects, which are observed in nonmagnetic semiconductors and some semiconductor devices in strong electric fields [19, 20, 30–32]. These are the MR effects caused by the magnetic field-dependent impact ionization. The field dependence was attributed to the Lorentz force deflecting the electron trajectories. In an applied magnetic field, the trajectories extend and, in bulk semiconductors, enhance inelastic scattering, which results in suppression of impact ionization [19]. In structurally asymmetric devices, this mechanism

causes the dependence of MR on the applied field polarity: magnetic fields of different signs deflect free carriers to the different areas of a device with different recombination rates [20]. Some authors believe that impact ionization at the Schottky barrier is responsible also for the observed large MR in metal/semiconductor [28] and metal/oxide/semiconductor structures [30]. It was suggested that the magnetic field shifts the acceptor levels at low temperatures, which facilitates localization of carriers and, consequently, suppresses impact ionization. Then, the observed MR behavior appears positive, monotonically changing upon the applied field variation, and symmetric relative to the magnetic field sign.

It is improbable that the latter mechanism is implemented in our case, despite the fact that our device is also based on the metal/oxide/semiconductor structure with the Schottky barrier. At the same time, there are strong grounds to believe that the impact ionization and magnetic-field effect on the carrier motion play the key role in the occurrence of the MR effect in the investigated structure. Indeed, in the zero-field I–V characteristic of the reverse-biased structure, we observe a sharp increase in the current at $|V_b| > 2$ V. This behavior can be interpreted as the autocatalytic impact ionization process. In an applied field, this feature is missing in the I–V characteristic; therefore, we may suggest that the magnetic field suppresses impact ionization. As we mentioned above, this can originate from deflection of the electron trajectories, which enhances the probability of electron recombination before they acquire the kinetic energy required for recombination. The recombination rate will be different for electrons deflected toward the SiO_2/p-Si interface containing many defects and in the bulk of a semiconductor containing few defects; in other words, it will depend on the magnetic field polarity. It is what we observed in our experiments. At high reverse bias voltages ($|V_b| > 2$ V), when, in our opinion, impact ionization occurs, the MR ratio has the largest values (Fig. 2). Obviously, the MR_{ph} value grows with the negative bias voltage value, because so does the electric field that accelerates electrons to the ionization threshold. Meanwhile, the applied magnetic field is sufficiently strong to suppress impact ionization via enhancement of recombination.

At all the rest V_b values, there are no features in the I–V characteristics that could be attributed to the effect of impact ionization; however, the MR effect, though weaker, is still observed, along with the current sensitivity to the magnetic field polarity. We believe that the field-induced conductivity change can still be explained by the change in the carrier recombination rate caused by deflection of the carrier trajectories toward the interface or in the bulk of a semiconductor. It is noteworthy that at $V_b > 0$, the MR_{ph} value can be either positive or negative, depending on the field value and sign; i.e. the magnetic field-induced variation of the carrier trajectories can not only enhance recombination, but, at certain H values, suppress it.

Now, let us analyze in more detail the above assumptions about the nature and behavior of the MR effect, taking into account the experimental geometry and the topology and energy structure of the device. It is convenient to analyze the photoconductivity features observed at different temperatures with the use of the schematic energy diagram, which illustrates the fundamental carrier transport processes occurring at the $Fe/SiO_2/p$-Si interface under optical radiation (Fig. 5). Taking into account the experimental geometry and the fact that photo-generated carriers are only created at the interface, it should be emphasized that the trajectories of photogenerated holes (at the forward bias) and photogenerated electrons (at the reverse bias) are localized near the SiO_2/p-Si interface (Fig. 6). The interface centers can work as the centers of recombination of photogenerated carriers. The recombination rate depends on the carrier type (electrons or holes) and on the charge state of the centers, i.e., on the Fermi level position relative to the energy levels of the centers, which, in turn, depends on temperature. Thus, the transport and magnetotransport properties of the device are determined by both the energy spectrum of the MIS junction right under to the metal electrode and the energy state of the interface centers located between the light spot and the Fe electrode.

Now, let us consider the forward-biased structure in zero magnetic field (Figs. 5a–5c and 6a). The excited electrons in Si near the interface move in the bulk of Si, while the simultaneously exited holes are accumulated in the Fe layer. In the forward-biased p-type semiconductor, the Schottky barrier for holes lowers or even completely vanishes, which ensures high photoconductivity of the device at $T > 40$ K. The interface centers with the energies much lower than E_F are charged by the electrons captured from the valence band and do not actively participate in recombination. At $T < 40$ K, the Fermi level E_F starts crossing the energy levels of the centers and electrons are released from them. The positively charged centers located under the metal electrode simultaneously capture electrons from the Fe layer and holes excited by light. The release and capture processes effectively suppress the photocurrent in the device. The device topology and experimental geometry are such that the trajectories of excited holes are parallel to the SiO_2/p-Si interface with the localized surface states. As the Fermi level E_F approaches the energy levels of the centers with decreasing temperature, recombination of holes on these centers enhances. Thus, below 40 K one should expect a significant increase in R_{ph}, which was observed by us (Fig. 1a). The nonmonotonic behavior of the $R_{ph}(T)$ curve at $T < 40$ K is apparently due to the features of the density of distribution of the surface states in the semiconductor band gap.

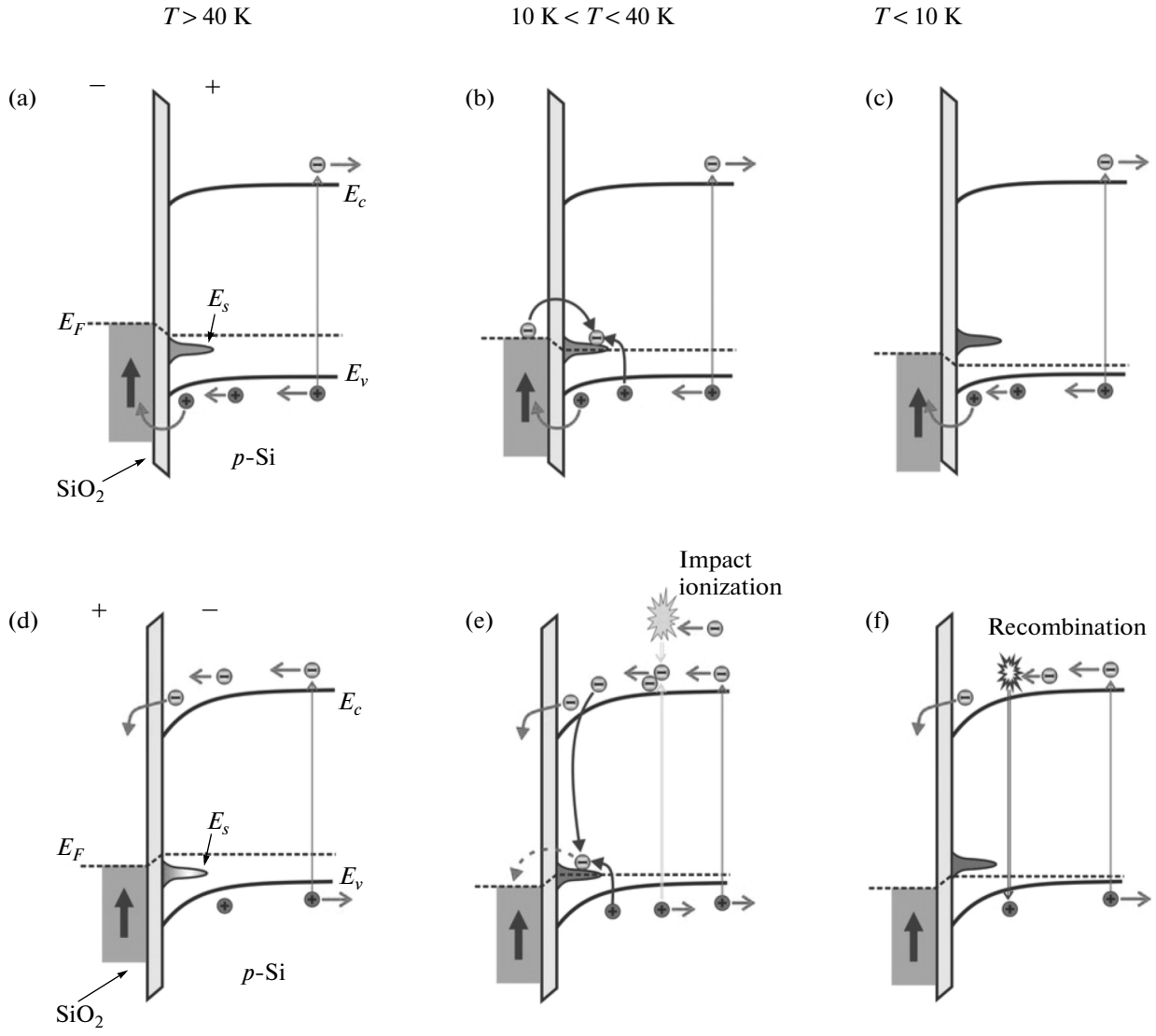

Fig. 5. Schematic diagrams illustrating the fundamental carrier transport processes at the MIS junction under optical radiation in the characteristic temperature ranges (a, d) $T > 40$ K, (b, e) $10 < T < 40$ K, and (c, f) $T < 10$ K. The diagrams correspond to (a–c) the forward and (d–f) reverse bias. The interface states participate more effectively in the carrier transport and recombination processes in the temperature range 10–40 K (b, e). Impact ionization resulting in the abrupt photocurrent growth occurs at a high reverse bias voltage (e). Recombination without participation of the interface states suppresses the photocurrent at low temperatures in the reverse bias regime (f).

So, what happens when the magnetic field is switched on? Our previous investigations of the magnetoimpedance of the $Fe/SiO_2/p$-Si structure showed that the field effect might be interpreted as the shift of the in-gap interface levels toward higher energies [11]. This could explain the shift of the characteristic features on the temperature dependence of R_{ph} observed by us at $H = +0.6$ T. However, this does not explain the strong dependence of R_{ph} on the field polarity. This effect was not observed in our magnetoimpedance measurements. Moreover, upon sweeping a positive magnetic field, first, we observe a slight decrease in the resistance and then the resistance starts growing (Fig. 3a and 4a), which is indicative of the competition between contributions of different mechanisms to the MR effect. We suggest the following scenario. Although the energy levels of the interface states shift in a magnetic field, this does not significantly change the R_{ph} value. We believe that the decisive role is played by the Lorenz force. The magnetic field with the direction taken by us as positive (parallel to the y axis) deflects the excited holes from the interface centers (see Fig. 6a). As a result, the carrier recombination rate drops and, when the field is switched on, we first observe the R_{ph} drop. Then, as the field increases, the distortion of the carriers trajectories extends the distance to be passed by electrons until they reach the metal electrode. The extended electron paths, in turn,

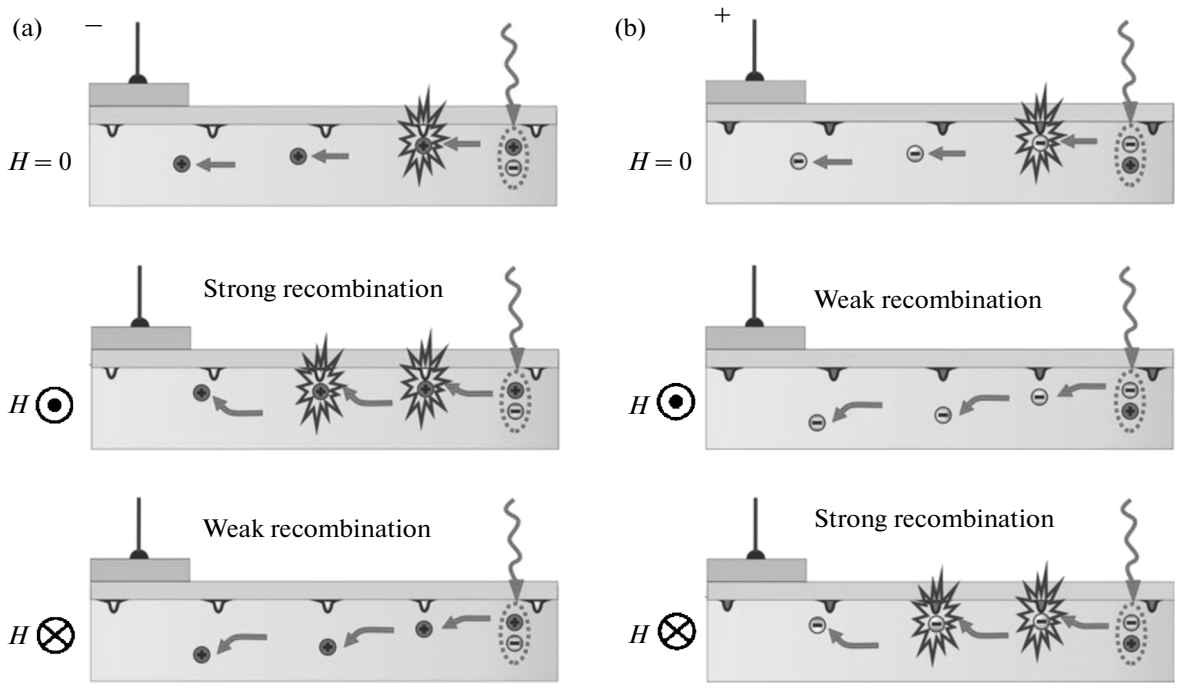

Fig. 6. Schematic of the photogenerated carrier transport in the device in zero magnetic field and in the fields of the opposite polarities at (a) forward and (b) reverse bias voltages. The magnetic field deflects carriers towards the interface, enhancing recombination due to the interface states.

enhance the probability of recombination of excited holes and, thus, increase R_{ph}.

In negative field H, the Lorentz force deflects holes toward the interface and facilitates recombination. As a result, R_{ph} rapidly grows. As we mentioned above, the recombination rate for holes on the interface centers is higher when the energy levels of the centers are close to the Fermi level E_F. Since E_F is proportional to the temperature, we may conclude that the peak in the $R_{ph}(T)$ dependence in the temperature range 10–30 K at the negative H values follows the in-gap distribution of the density of interface states.

Let us pass to the reverse-biased structure (Figs. 5d–5f and 6b). Here, the charge is carried by photoexcited electrons along the SiO_2/p-Si interface between the light spot and the metal electrode. Since in a p-type semiconductor electrons are the minority carriers, the interface states still do not work ($T > 40$ K) and R_{ph} is significantly higher than at the forward bias. In our opinion, below 40 K at $H = 0$ the resistance behavior is governed by several mechanisms. First, the interface states come into play: the positively charged centers can simultaneously capture electrons from the conduction band and holes from the valence band. This process should suppress the photocurrent in the device. Meanwhile, the electrons captured by the centers localized under the metal electrode can tunnel into the metal electrode before the hole is captured by the center from the valence band and recombination occurs. Obviously, activation of such an additional conductive channel should reduce R_{ph}. However, we believe that at the reverse bias the key role in the reduction of R_{ph} below 40 K is played by impact ionization. When the reverse bias exceeds the threshold value $V_b = -1.5$ V at $T = 20$ K, the kinetic energy of the electrons surpasses the ionization energy and impact ionization is triggered, which is accompanied by the abrupt electric current growth in the device (Fig. 2a), i.e., by a decrease in R_{ph}.

As in the forward-biased structure, the magnetic field effect is reduced to deflection of the electron trajectories. At $H < 0$, the Lorentz force deflects electrons from the SiO_2/p-Si interface, thereby extending the electron trajectories. These extended trajectories enhance the probability of recombination of exited electrons. Therefore, one can observe a minor increase in R_{ph} regardless of impact ionization, which occurs at $T < 40$ K and does not occur at $T > 40$ K. At the opposite field direction ($H > 0$), electrons are deflected toward the interface where the recombination rate is higher than in the bulk of semiconductor. Recombination becomes especially intense when the interface states start releasing electrons and thereby transform to the effective recombination centers. Since the fast recombination suppresses impact ionization, in this region we observe a sharp increase in R_{ph} in an applied positive magnetic field. The strongest R_{ph} variations at 15–35 K (peak in the $R_{ph}(T)$ curve at $H = +0.6$ T) are

apparently related to the shape of the distribution function of the interface states and to the fact that recombination is effective on the centers whose energy levels are in the close proximity to E_F. Some discrepancy between the $R_{ph}(T)$ peak positions at negative H values under the forward bias and at positive H values under the reverse bias can be explained by the fact that the energy levels of the interface states follow the shift of the allowed bands in the semiconductor to the interface upon structure bias variation, while the Fermi level position remains invariable. In other words, at a fixed temperature, the distances between the E_F level and the center of the interface state density distribution are different at different biases across the device.

The results obtained in other experimental geometries are consistent with the proposed scenario of the magnetic field effect on photoconductivity of the device under study. When the position of the laser spot along the y axis is changed (distance x_0 to the Fe electrode is constant) at all other experimental conditions being equal, neither the transport properties nor the R_{ph} and MR_{ph} absolute values change. A decrease in x_0 does not cause any substantial changes in the curves either, but strongly affects the resistance and MR values: R_{ph} increases and MR_{ph} decreases (Fig. 4). This is quite natural, since the trajectories of photoexcited carriers, starting with the laser spot and ending with the metal electrode, shorten and the recombination probability lowers. Consequently, suppression of the photocurrent by recombination weakens.

When a magnetic field is applied along the x direction, the MR effect remains noticeable, yet significantly weakened. The point is that in this geometry the Lorenz force deflecting the carrier trajectories toward the interface or in the bulk of semiconductor is negligible, because it is actually determined by the small carrier velocity projection onto the y axis.

In the framework of the proposed model, we still do not quite understand the sharp R_{ph} growth at the reverse bias below 10 K in zero field and even sharper R_{ph} growth in nonzero magnetic fields of any polarity. Perhaps, one should take into account the occurrence of additional recombination channels. Recall that the current mainly flows right next to the insulator/semiconductor interface, containing various defects, which can be activated at lower temperatures and start suppressing impact ionization, thus leading to the resistance growth. The role of the magnetic field can be reduced to deflection of the carrier trajectories and modification of the energy spectrum of defects. Anyway, the observed R_{ph} behavior needs more thorough analysis. However, we believe that our simple model covers the most relevant points of the optically induced MR effect in the $Fe/SiO_2/p$-Si-based device.

CONCLUSIONS

It was shown that the extremely high magnetoresistance can be induced in the device based on the $Fe/SiO_2/p$-Si structure by laser radiation. The magnetoresistance ratio can be controlled in a wide range by a bias voltage across the device. Moreover, the optically induced magnetoresistive effect strongly depends on the magnetic field polarity. The main features in the behavior of photoconductivity of the device in a magnetic field can be explained using the model proposed by us. According to our model, the magnetic field effect on the transport properties of the structure under study can be related to the Lorentz force acting on photogenerated carriers. Deflection of the carrier trajectories by a magnetic field enhances the probability of recombination and, thus, reduces the photoconductivity. The asymmetric magnetic field effect on the photoconductivity was attributed to the difference in the carrier recombination rates at the oxide-silicon interface and in the bulk of silicon. Depending on the field direction, carriers are deflected either toward the interface or away from it, which yields different effective photoinduced currents in the device at the opposite magnetic field polarities. The dependence of the MR ratio on the bias voltage across the device is also caused by distortion of the carrier trajectories, but here the electric field plays different role, accelerating the carriers. At high voltages, the magnetoresistance mechanism starts acting on electrons: the impact ionization is switched on, which can be suppressed by the increasing magnetic field extending the electron trajectories and enhancing recombination. In the impact ionization mode, the device exhibits the strongest magnetoresistive effect.

We believe that the silicon-based devices with the resistance controlled by the three parameters, including optical radiation, magnetic field, and bias voltage have the high application potential. Compatibility of such devices with the highly developed silicon technology makes it possible to easily integrate them in silicon chips for achieving high functionality by means of the interplay between the electronic, optoelectronic, and magnetic responses.

ACKNOWLEDGMENTS

This work was supported by the Russian Foundation for Basic Research, project nos. 14-02-00234-a and 14-02-31156; the Russian Ministry of Education and Science, state task no. 16.663.2014K; and the Russian Ministry of Education and Science, project no. 02.G25.31.0043.

REFERENCES

1. A. Fert, Phys. Usp. **51**, 1336 (2008).
2. B. Behin-Aein, D. Datta, S. Salahuddin, and S. Datta, Nature Nanotechnol. **3**, 97 (2008).

3. S. I. Kiselev, J. C. Sankey, I. N. Krivorotov, N. C. Emley, R. J. Schoelkopf, R. A. Buhrman, and D. C. Ralph, Nature (London) **425**, 380 (2003)
4. Y. Suzuki and H. Kubota, J. Phys. Soc. Jpn. **77**, 031002 (2008)
5. N. Volkov, G. Petrakovskii, P. Boeni, E. Clementyev, K. Patrin, K. Sablina, D. Velikanov, and A. Vasiliev, J. Magn. Magn. Mater. **309**, 1 (2007).
6. B. Dieny, in *Magnetoelectronics,* Ed. by M. Johnson (Elsevier, Amsterdam, 2004).
7. J. S. Moodera and R. H. Meservey, in *Magnetoelectronics*, Ed. by M. Johnson (Elsevier, Amsterdam, 2004).
8. P. Ciureanu, L. G. C. Melo, D. Seddaoui, D. Menard, and A. Yelon, J. Appl. Phys. **102**, 073908 (2007).
9. K. Hika, L. V. Panina, and K. Mohri, IEEE Trans. Magn. **32**, 4594 (1996).
10. S. Xiao, Y. Liu, Y. Dai, L. Zhang, S. Zhou, and G. Liu, J. Appl. Phys. **85**, 4127 (1999).
11. N. V. Volkov, A. S. Tarasov, E. V. Eremin, A. V. Eremin, S. N. Varnakov, and S. G. Ovchinnikov, J. Appl. Phys. **112**, 123906 (2012).
12. R. Jansen, Nature Mater. **11**, 400 (2012).
13. S. P. Dash, S. Sharma, R. S. Patel, M. P. de Jong, and R. Jansen, Nature (London) **462**, 491 (2009).
14. S. A. Crooker, M. Furis, X. Lou, D. L. Smith, C. Adelmann, C. J. Palmstrom, and P. A. Crowell, J. Appl. Phys. **101**, 081716 (2007).
15. J. E. Hirsch, Phys. Rev. Lett. **83**, 1834 (1999).
16. Y. A. Bychkov and E. I. Rashba, JETP Lett. **39**, 78 (1984).
17. G. Dresselhaus, Phys. Rev. **100**, 580 (1955).
18. M. Cardona, N. E. Christensen, and G. Fasol, Phys. Rev. B **38**, 1806 (1988).
19. J. Lee, S. Joo, T. Kim, K. H. Kim, K. Rhie, J. Hong, and K.-H. Shin, Appl. Phys. Lett. **97**, 253505 (2010).
20. S. Joo, T. Kim, S. H. Shin, J. Y. Lim, J. Hong, J. D. Song, J. Chang, H.-W. Lee, K. Rhie, S. H. Han, K.-H. Shin, and M. Johnson, Nature **494**, 72 (2013).
21. M. Delmo, S. Yamamoto, S. Kasai, T. Ono, and K. Kobayashi, Nature (London) **457**, 1112 (2009).
22. C. Wan, X. Zhang, X. Gao, J. Wang, and X. Tan, Nature (London) **477**, 304 (2011).
23. N. V. Volkov, A. S. Tarasov, E. V. Eremin, F. A. Baron, S. N. Varnakov, and S. G. Ovchinnikov, J. Appl. Phys. **114**, 093903 (2013).
24. N. V. Volkov, C. G. Lee, P. D. Kim, E. V. Eremin, and G. S. Patrin, J. Phys. D: Appl. Phys. **42**, 205009 (2009).
25. Z. J. Yue, K. Zhao, H. Ni, S. Q. Zhao, Y. C. Kong, H. K. Wong, and A. J. Wang, J. Phys. D.: Appl. Phys. **44**, 095103 (2011)
26. N. V. Volkov, A. S. Tarasov, E. V. Eremin, S. N. Varnakov, S. G. Ovchinnikov, and S. M. Zharkov, J. Appl. Phys. **109**, 123924 (2011).
27. M. A. Green, F. D. King, and J. Shewchun, Solid State Electron. **17**, 551 (1974).
28. B. I. Shklovskii and A. L. Efros, *Electronic Properties of Doped Semiconductors* (Springer, Berlin, Heidelberg, 1984).
29. M. M. Parish and P. B. Littlewood, Nature **426**, 162 (2003).
30. Z. G. Sun, M. Mizuguchi, and H. Akinaga, Appl. Phys. Lett. **85**, 5643 (2004).
31. C. Ciccarelli, B. G. Park, S. Ogawa, A. J. Ferguson, and J. Wunderlich, Appl. Phys. Lett. **97**, 082106 (2010).
32. J. J. H. M. Schoonus, F. L. Bloom, W. Wagemans, H. J. M. Swagten, and B. Koopmans, Phys. Rev. Lett. **100**, 127202 (2008)